

An algorithm for crowded stellar fields analysis

E. Diolaiti¹, O. Bendinelli¹, D. Bonaccini², G. Parmeggiani³, F. Rigaut²

¹ Bologna University Astronomy Department

² European Southern Observatory

³ Bologna Astronomical Observatory

ABSTRACT

We report the work in progress on a method to analyze Adaptive Optics images of stellar fields, using as an approximation of the instrumental PSF an intensity map extracted directly from the field. The basic working hypotheses are that the PSF is constant in the image sections analyzed and that the residual background irregularities are modeled by a linear fitting on sub-frames patches of a few diffraction rings in size.

A first list of local intensity spikes is created for stars detection; each maximum is then cross-correlated with the PSF and, if a sufficiently similarity is found, the reliable identification of the star along with the determination of its position (with sub-pixel accuracy) and relative intensity are achieved with an iterative procedure which fits a sub-image centered on the object under examination with a superposition of shifted scaled PSFs.

After describing the algorithm performances on simulated cases, an application to a K-band PUEO image of the Galactic Center is shown.

1. Introduction

The analysis of a crowded stellar field generally involves stars detection, astrometry and photometry. The quality of the results is characterized by various parameters, depending on the scientific purpose of the observations: stellar population studies require high dynamic range (completeness limit) and reliable photometry, whereas the analysis of stars kinematics is based on the most accurate astrometry. The results that can be achieved with the observation and the analysis of a stellar field are both instrument and software dependent. From an instrumental point of view the limiting factors are the spatial resolution, more and more important as the crowding of the field increases, and the photometric dynamic range.

If there is no strong background feature a stellar field may be considered as a sum of point-like sources; the observed image appears essentially as a superposition of shifted scaled replicas of the Point Spread Function. An algorithm might exploit this *a priori* knowledge.

The most commonly used tool in stellar fields analysis is DAOPHOT (Stetson 1987), originally developed for ground-based seeing-limited observations. DAOPHOT uses “shape” parameters to identify objects and an analytical model of the PSF to determine stars positions and approximate magnitudes; the deviations of the actual PSF from the model are included in a residual map which is used to refine the photometry. This semi-analytical approach seems to be perfectly justi-

fied for seeing-limited observations, characterized by a wide smooth and easily parametrizable PSF.

In diffraction-limited imaging (HST, Adaptive Optics) the great enhancement of spatial resolution allows the separation of very crowded groups of stars, but there are also some drawbacks in post-processing because of the detailed structure of the PSF. Sosin & King (1997) have proposed a modification of DAOPHOT to avoid false detections in HST images analysis. Esslinger and Edmunds (1998) show how irregular PSF features due to the adaptive optics partial compensation of the atmospheric turbulence may affect the photometry of faint stars in the field.

For these reasons it seems worth trying to create an algorithm which takes into consideration the specificity of the AO response.

2. Algorithm description

2.1 General remarks

The algorithm in its present form treats the image essentially as a superposition of shifted scaled replicas of the input PSF. This approximation is acceptable if the instrumental response is space-invariant and the image is a *pure stellar field* without other complex features. In practice the latter condition may be slightly relaxed: any smooth background emission is approximated with a simple local background in the form of a slanting plane (see Sect. 2.4).

The starting point for the algorithm is a list of local maxima sorted in order of decreasing intensity and assumed to represent *suspected stars*. Each object that *matches* the PSF is analyzed and its parameters (position and intensity) are determined, taking into consideration the crowding effects due to surrounding brighter stars: the underlying strategy is that the contribution of neighboring fainter objects may be initially neglected. If a star is near a fainter one, its parameters will be refined subsequently, when the latter will be examined in turn. As a new object is detected it is added to an *image model*, which represents a fundamental reference in the subsequent analysis of fainter local maxima. The last step is a search for *hidden stars* (e.g. close binaries).

2.2 PSF determination

The estimation of the PSF has a fundamental importance. It may be obtained from the observation of a point-like source or be reconstructed using statistical wavefront sensor data (Véran *et al.* 1997) provided all the field analyzed is isoplanatic around the wavefront sensor guide star. If no such approximation is available, it is necessary to extract it directly from the frame, e.g. by superposing the images of some suitable stars in the field with a shift-and-add (SAA) algorithm (e.g. Christou & Bonaccini 1996). The extracted PSF should be as extended as possible to reproduce accurately the haloes of bright stars. Very extended haloes, not reproduced by a truncated PSF, are approximated by a local background (Sect. 2.4). When no isolated object is available for determining the PSF one may choose some sufficiently bright stars contaminated just by fainter objects, whose contribution may be determined and subtracted with a local analysis based on a preliminary rough approximation of the PSF; the resulting decontaminated stellar images may then be superposed by shift-and-add.

2.3 Search for local maxima

The list of suspected stars is simply obtained by searching for the image local maxima (pixels brighter than their 8-neighbors) above a given threshold. A rough choice for the detection threshold is the central intensity of the faintest discernible star in the frame. If the image background b and its standard deviation σ_b are known, the threshold may be chosen equal to $b+k\sigma_b$, for some value of k .

2.4 Analysis of detected maxima

The first step for each detected maximum is to extract a sub-image $i(x, y)$ from the original frame, centered on the maximum itself; the sub-image size may be of the order of one or two diffraction rings, in any case smaller than the truncated PSF size. Then the image model local contribution is subtracted: if the object under examination is a secondary maximum of an already detected (i.e. brighter) star, the residual sub-image $i_r(x, y)$ will have no central spike left. Otherwise the remaining local maximum is *cross-correlated* with the PSF (typically the diffraction core) in order to have an objective comparison with a reference stellar image. Before being cross-correlated, the residual sub-image and the PSF $p(x, y)$ are centered on their maximum intensity pixels; centering is performed with sub-pixel accuracy, by means of an iterative Fourier shift which tends to reduce the distance of the data centroid from a fixed position (the middle of a given pixel), as explained by Christou & Bonaccini (1996).

The cross-correlation between the central spike in the residual sub-image and the PSF core is defined as

$$c = \frac{\sum_{x,y} i_r(x, y)p(x, y)}{\sqrt{\sum_{x,y} i_r^2(x, y)} \sqrt{\sum_{x,y} p^2(x, y)}} \quad (2.4.1);$$

if it is greater than a fixed threshold (e.g. 0.7 or 0.8), the sub-image $i(x, y)$ is *fitted* with a model consisting essentially of a superposition of shifted scaled replicas of the PSF. Crowding effects are handled as follows: known (i.e. brighter) stars laying within the image box are fitted along with the local maximum under examination (multiple fitting), the halo contribution of already detected stars outside the box is included as a fixed additive term kept constant in the estimation, fainter (thus still unexamined) objects are neglected and will be analyzed later. In mathematical terms the fitting model is

$$h(x, y) = i_0(x, y) + \sum_{n=1}^{N_s} c_n p(x - x_n, y - y_n) + b_0 + b_1 x + b_2 y \quad (2.4.2),$$

where $i_0(x, y)$ is the fixed additive contribution due to stars outside the sub-image support, known from the image model, N_s is the number of point-like sources in the box, x_n, y_n, c_n are the parameters (sub-pixel accuracy position and flux) for the n -th star, $p(x - x_n, y - y_n)$ is the PSF shifted in the position of the n -th source and b_0, b_1, b_2 are the coefficients defining the local background. The PSF is shifted applying the properties of Fourier transforms:

$$p(x - x_n, y - y_n) = FT^{-1} \left\{ FT \{ p(x, y) \} e^{-i2\pi(u x_n + v y_n)/N} \right\} \quad (2.4.3),$$

where FT is the discrete Fourier transform operation, N is the sub-image size in pixels and u, v are Fourier spatial fre-

quencies. The application of Fourier transforms to shift a discrete image by an arbitrary amount is justified when the critical sampling condition is fulfilled, as usual in AO imaging.

In general a superposition of shifted replicas of a truncated PSF does not support the whole image being fitted: the data are masked to prevent fitting of regions not covered by the model. Masking of each shifted replica of the PSF is suitable to eliminate the small amount of light spread outside the PSF support because of the oscillations introduced by Fourier interpolation.

The parameters are estimated by minimization of the least square error between the model $h(x, y)$ and the sub-image $i(x, y)$. The optimization technique is an iterative regularized Newton scheme with linearized Hessian (also known as Marquardt method); the stopping condition is that the variation of the parameters between successive iterations is smaller than a fixed tolerance. The fitting algorithm is very fast: it typically converges in about 10 iterations.

If the central maximum is not a star the fitting procedure generally produces anomalous results: it may not converge at all, the presumed object may have an estimated negative intensity or its position may converge toward another true star. In all these cases the fit is considered unacceptable and the maximum is rejected. Otherwise it is accepted as a new detected star and it is added to the image model.

We are in the process of quantifying this fitting procedure performance with pre-defined parameters.

A further optional check may be included to prevent false detection of irregular features on diffraction rings, mainly due to ring fragmentation (see Fig. 1). These local maxima are generally recognized and rejected with the previous tests and operation, but sometimes they may be accepted as stellar objects. For each detected star the optional check consists of a search for a neighboring brighter object that may be considered (both for distance and flux ratio) the central spike of a diffraction pattern having the examined object itself as a ring feature. If the search is successful the maximum may be rejected or marked as a suspected secondary diffraction spike. This check is very useful especially when the approximation of the PSF is not extended enough.

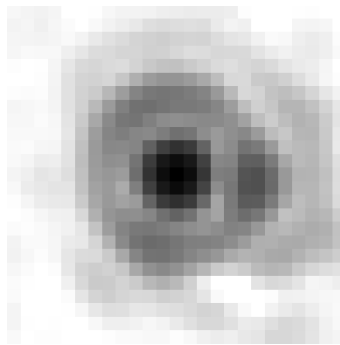


Figure 1. Observed ADONIS PSF in K-band. Grey levels are in $\log(1+I)$ scale.

As explained above the starting point for the algorithm is a list of local maxima. In this way relatively faint stars in very crowded groups may be lost, because their spikes are *hidden* by the contamination of brighter objects. The search for these stars is performed by extracting a sub-image centered on each detected object and subtracting the image model local con-

tribution. If a maximum comes out, it is checked with cross-correlation and possibly analyzed. The search is repeated iteratively for a given sub-image until no more hidden maximum is found.

In the usual presence of multiple images of the same field, a cross-check of the detected stars between images sub-frames will ensure a high degree of trust in the results, as the detection errors will be minimized.

3. Testing the algorithm

3.1 General remarks

Tests have been performed on synthetic images, created with a numerically simulated ADONIS PSF in K band, representing a long exposure (10 sec) image of a K0-type star with $V = 6$ mag, observed in $0''.62$ seeing conditions; the assumed guide star for the observation is the target itself and, given its bright V magnitude, the RETICON 200 Hz wavefront sensor is used. The final simulated PSF (Fig. 2) is a 128×128 array, it is critically sampled at K-band (pixel size $\cong 31.5$ mas) and has a Strehl ratio of about 0.46.

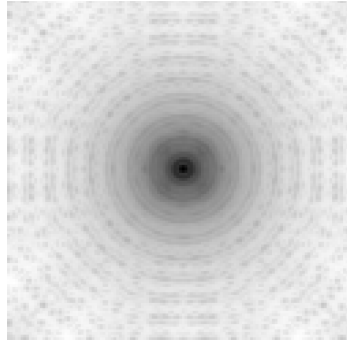


Figure 2. ADONIS synthetic PSF in K-band. Grey levels are in $\log(1+I)$ scale.

Each image has been generated by convolving this PSF with a set of δ -functions at fixed positions and relative intensities, applying Fourier transforms to perform sub-pixel shifts. Poissonian-like noise and gaussian background noise have been added: the former has been generated multiplying the square root of the image by an array of pseudo-random numbers extracted from a standard gaussian distribution, the latter is represented by an array of pseudo-random numbers from a gaussian distribution of given mean b and standard deviation σ_b .

The signal to noise ratio (SNR) of a simulated frame has been characterized referring to the central intensity I of a given star (the faintest or the brightest one depending on the particular situation) and has been defined as

$$SNR = \frac{I}{\sqrt{\sigma_p^2 + \sigma_b^2}} \cong \frac{I}{\sqrt{(I-b) + \sigma_b^2}} \quad (3.1.1),$$

where $\sigma_p \cong \sqrt{I-b}$ and σ_b are the standard deviations for Poisson and gaussian background noise respectively. In general two different SNR situation have been investigated (e.g. $SNR = 50$ and $SNR = 10$).

3.2 Testing the fitting procedure

The first battery of tests concerns the fitting algorithm. The target image is a 16×16 array with 4 stars at fixed positions and with intensity ratios of 1:2, 1:5 and 1:10 respectively. In practice we have generated sets of 50 frames, differing by the additive noise term. An 11×11 truncated PSF (including the central spike and the first diffraction ring) has been contaminated with noise and used in the fit. Estimated positions (in pixels) and relative magnitudes have been compared with the true values computing the corresponding residuals. As obvious the dispersion increases for faint stars or in poor SNR condition. Figures 3 and 4 show the residuals for a set of 50 noisy frames having a $SNR = 50$ at the brightest star peak. The photometric errors are completely uncorrelated, whereas the position of the faintest star is slightly biased (about 1/5 pixels). We interpret this effect as due to the truncation of the PSF: the faintest source is approximately on the border of the PSF centered at the brightest star position. However this aspect has to be investigated in greater detail. The astrometric bias seems to disappear when fitting more noisy images ($SNR = 10$) and this is quite intriguing.

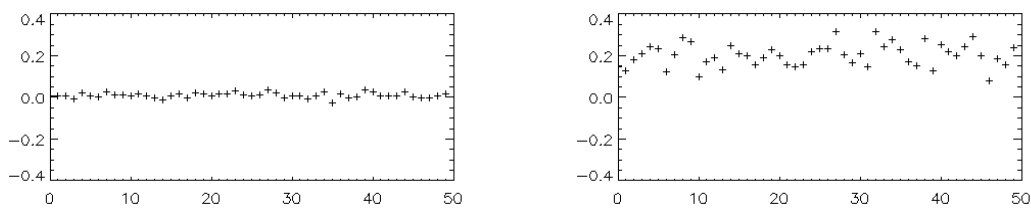


Figure 3. Typical coordinate residuals (in pixels) for the brightest star (left) and the faintest one (right) in the test image.

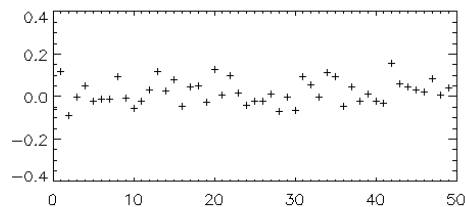


Figure 4. Residuals for the magnitude difference between the brightest star and the faintest one in the test image.

As the fitting algorithm requires an initial estimate of the point-like sources positions, it is interesting to study the dependence of the solution on these estimates. For this purpose we have fitted some of the images used in the previous tests starting from different initial positions within a distance of about 1.5 pixels from the true values and we have verified that the algorithm converges always to the same solution.

3.3 Simulations of two-component images

The algorithm for stellar fields analysis has been tested on simulated images of “binary stars” characterized by different separations and relative magnitudes. We have considered the following cases:

- type 1: close binary star at the Rayleigh limit (separation $0''.126$)

- type 2: star on the diffraction ring of a brighter one (separation $0''.190$)
- type 3: faint star in the halo of a much brighter one (separation $0''.700$).

Each case has been divided into sub-cases corresponding to a different relative magnitude. A systematic completeness study is still in progress. For each situation we have analyzed a set of 50 noisy frames using a noisy truncated PSF. For simplicity we refer here to three typical situations: a type 1 example with magnitude difference 0.753 (intensity ratio 2:1), a type 2 example with magnitude difference 1.747 (intensity ratio 5:1) and a type 3 example with magnitude difference 3.252 (intensity ratio 20:1). The detection rate for the secondary component is always 100% in these cases. The astrometry of the brighter component is very accurate, with errors of a few *mas*, whereas the residuals for the secondary stars are affected by a larger dispersion and some errors. The plots show an astrometric bias (Fig. 5, left) ranging from about 0.1 pixels ($0''.003$) for the close binary (smallest separation and magnitude difference) to about 0.2-0.3 pixels ($0''.007$) for the faint star in the halo (largest separation and magnitude difference). There is a photometric bias (Fig. 5, right) ranging from a few hundredths of magnitude (closest binary) to about 0.1-0.2 mag (type 2 and 3 binaries).

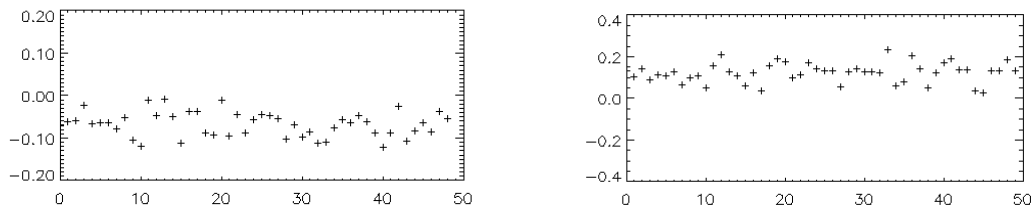


Figure 5. Left: y coordinate residuals for the close binary secondary component. Right: relative magnitude residuals for a type 2 binary.

The reported errors are not huge but should be understood and corrected, if possible. The observed biases may be due to the fitting method (linearization of the Hessian, too heavy regularization) or simply to the restricted approximation of the PSF used in the analysis. These aspects are under investigations.

3.4 Simulation of a stellar field

We have generated a synthetic frame (Fig. 6) with 135 stars and a photometric dynamic range of 7 mag, using stellar positions and relative magnitudes from the HST data of a Globular Cluster. Additive noise contamination has been included. The PSF used in the analysis has been extracted from the field: it is a combination of the brightest star in the frame (after subtracting the contribution of some fainter objects determined with a preliminary approximation of the PSF) and the mean SAA image of the inner part of some other suitable stars. It includes the central spike and four diffraction rings. In practice we have used the whole PSF to build up the image model (see Sect. 2.1), whereas the local fitting has been performed with a restriction extending out to the first diffraction ring.

Even if the synthetic stellar field is not crowded globally ($4 \text{ stars} \times \text{arcsec}^{-2}$) it contains many local “difficult” situations, with close binaries and groups of stars separated by distances comparable to the radius of the inner diffraction ring.

The 126 detected objects are reported in Figure 6. Some stars (9) have been lost, but they are always faint and in very close

binaries or in the halo of the brightest objects with a great magnitude difference (4-5). We still have a few false detections, however limited to faint maxima in extended haloes or in the background noise.

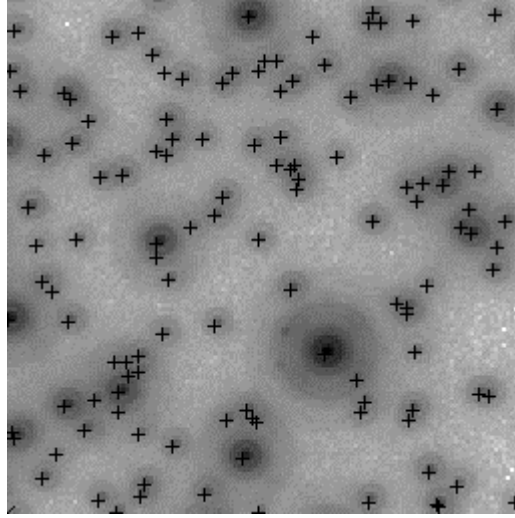


Figure 6. Simulated stellar field. Crosses represent detected stars. Grey levels are in $\log(1+I)$ scale.

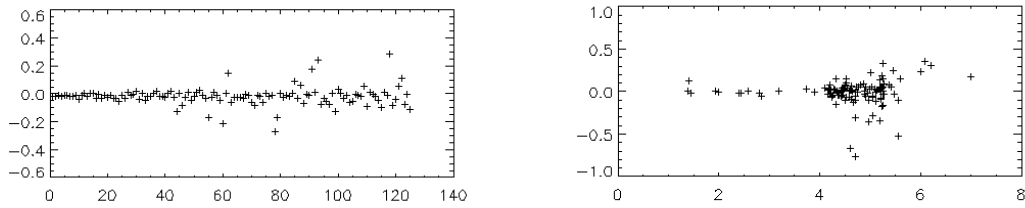


Figure 7. Left: y coordinate residuals (in pixels) for the detected stars. Right: relative magnitude residuals vs. relative magnitudes.

Apart from some cases, the astrometric errors are always smaller than 0.1-0.2 pixels (3-7 mas) and the relative magnitude residuals are within 0.5 mag (Fig. 7). Moreover no magnitude-dependent bias is present.

We plan to analyze different replicas of the same simulated field differing for the additive noise contamination, in order to characterize statistically the detection reliability as well as the astrometric and photometric accuracy.

4. Application to a real case: the Galactic Center

The algorithm has been run on a K-band PUEO image of the Galactic Center (Fig. 8); the total field of view is about $13 \times 13 \text{ arcsec}^2$ with a pixel size of 0.035 arcsec. The PSF for the analysis is a SAA superposition of three bright stars previously “decontaminated” with the procedure described in section 2.2 and it includes the inner core and the first two rings of the diffraction pattern. The 669 detected stars are marked by crosses on Fig. 8. The derived luminosity function (Fig. 9) extends over a dynamical range of more than 11 mag.

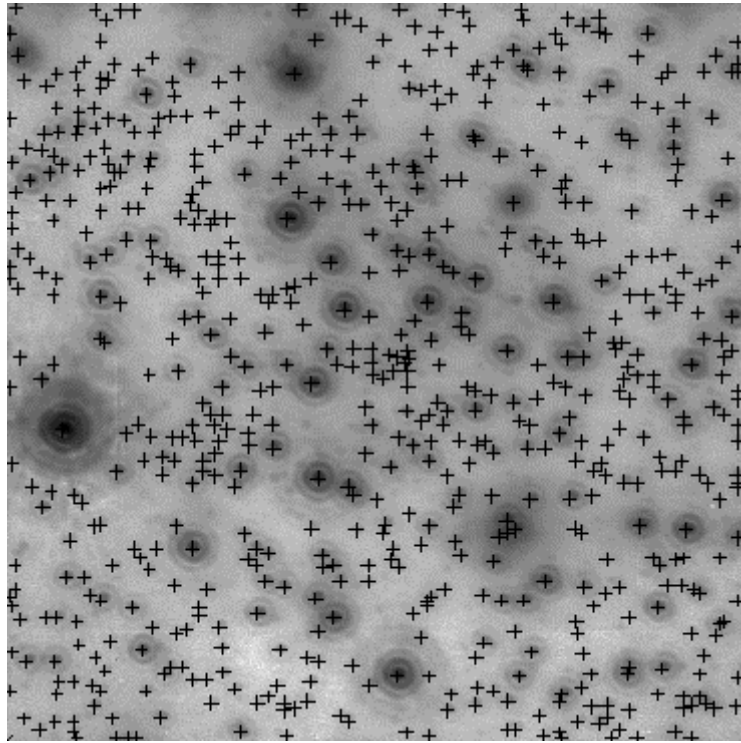


Figure 8. Galactic Center. Crosses represent detected stars. Grey levels are in $\sqrt[4]{\log(1+I)}$ scale.

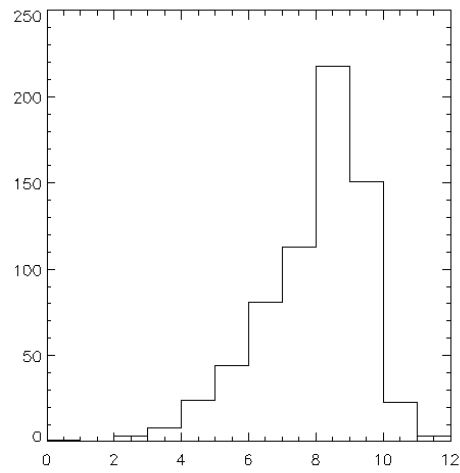


Figure 9. Luminosity function of detected stars in the Galactic Center. Horizontal axis: relative magnitudes. Vertical axis: number of stars.

5. Conclusions and future work

According to our simulations the algorithm seems to work quite well. Lost stars are faint and positioned in the halo of much brighter objects; false detections are limited to faint spikes dispersed in extended haloes or in the background; close binaries are successfully detected for reasonable separation and magnitude difference. The method, coded in IDL, is also fast: the analysis of the synthetic field (with about 350 initial maxima and more than 120 detected stars) requires about 10-15 minutes on a 200 MHz Pentium PC with Lynux operative system. For a given degree of crowding of the input field, the limiting factor for speed is essentially the size of the sub-image chosen for the local fit around each suspected star.

Our main goals for the future are to improve the algorithm, especially trying to understand and correct the observed biases, and to fully characterize it, in terms of reliability of detection, astrometric and photometric accuracy, completeness limit for various degree of crowding. The characterization will also involve a comparison with other methods, as DAOPHOT and a deconvolution algorithm recently proposed by Véran & Rigaut (1998). Multiple images of the same crowded stellar field, obtained with a time-varying PSF, might be analyzed in order to see how it is possible to exploit multiple observations to reduce the detection errors for faint stars. Finally we want to study the influence of the PSF variation on the analysis and, if it will be necessary, we will try to modify our method in order to take into proper consideration the effects of anisoplanatism.

References

- Stetson P., 1987, PASP, 99, 191
- Sosin C., King I.R., 1997, AJ, 113(4), 1328
- Esslinger O., Edmunds M.G., 1998, A&A Suppl. Ser., 129, 617
- Véran J.-P., Rigaut F., Maitre H., Rouan D., 1997, J. Opt. Soc. Am. A, 14(11), 3057
- Christou J.C., Bonaccini D., 1996, in Technical Report ESO VLT Doc. No. GEN-TRE-ESO-11620-1261
- Véran J.-P., Rigaut F., 1998, Proc. SPIE 3353, 426